Novel enzymatic synthesis of spacer-linked Pk trisaccharide targeting for neutralization of Shiga toxin

Novel enzymatic synthesis of spacer-linked P^k trisaccharide targeting for neutralization of Shiga toxin

Tatsuya Kato[a,b,c], Takahiro Oizumi[a], Makoto Ogata[d], Akiko Murakawa[c], Taichi Usui[c], Enoch Y. Park[a,b,c*]

[a] *Laboratory of Biotechnology, Department of Applied Biological Chemistry, Faculty of Agriculture, Shizuoka University, 836 Ohya, Suruga-ku, Shizuoka 422-8529, Japan*

[b] *Laboratory of Biotechnology, Green Chemistry Research Division, Research Institute of Green Science and Technology, Shizuoka University, 836 Ohya Suruga-ku, Shizuoka 422-8529, Japan*

[c] *Laboratory of Biotechnology, Integrated Bioscience Section, Graduate School of Science and Technology, Shizuoka University, 836 Ohya, Suruga-ku, Shizuoka, 422-8529, Japan*

[d] *Department of Chemistry and Biochemistry, Fukushima National College of Technology, 30 Nagao, Iwaki, Fukushima 970-8034 Japan*

[*] Corresponding author at: Green Chemistry Research Division, Research Institute of Green Science and Technology, Shizuoka University, 836 Ohya Suruga-ku, Shizuoka 422-8529, Japan. Tel. & Fax: +81 54 238 4887. *E-mail address:* acypark@ipc.shizuoka.ac.jp (Enoch Y. Park).

ABSTRACT

A novel alkyl spacer-conjugated derivative of P^k trisaccharide (P^k), one of the active receptors of Shiga toxins (Stxs; Stx1 and Stx2) produced by pathogenic *Escherichia coli* (STEC), was designed and synthesized by a combination of cellulase-mediated condensation from *Trichoderma reesei* and α1,4-galactosyltransferase (LgtC) from *Neisseria gonorrhoeae.* The specific activity of *N. gonorrhoeae* LgtC was 66 U/mg, which was 13-fold higher than that from *N. meningitidis* expressed in *E. coli*. 5-Trifluoroacetamidopentyl-β-P^k (TFAP-P^k) was synthesized (yield of 86%, based on the amount of TFAP-lactose added) and its binding to Stx1a-B and Stx2a-B was evaluated. The dissociation constants (K_{DS}) of Stx1a-B and Stx2a-B to the spacer-linked P^k, immobilized on a CM5 sensor chip, were 6.8×10^{-6} M ($k_{on} = 4.1 \times 10^{1}$ $M^{-1}S^{-1}$, $k_{off} = 2.8 \times 10^{-4}$ S^{-1}) and 2.2×10^{-5} M ($k_{on} = 3.9 \times 10^{2}$ $M^{-1}S^{-1}$, $k_{off} = 8.6 \times 10^{-3}$ S^{-1}), respectively. This result suggests that the monovalent P^k-derivative, conjugated to a pentylamino group, represents a promising Stx-neutralizing agent. This cellulase-mediated condensation using cellulase and glycosyltransferase is a valuable tool for the synthesis of spacer-linked oligosaccharide.

Keywords: α1,4-Galactosyltransferase; Shiga toxin; Globotriose; *Neisseria gonorrhoeae*; Cellulase-mediated condensation

1. Introduction

Cell surface glycans are involved in many physiological phenomena, including cell differentiation, cell development, signal transduction, virus and pathogen infection, and cancer metastasis. Glycan-binding proteins (GBPs) have crucial roles in these phenomena by recognizing and binding specific glycans. This GBP-glycan interaction is comparatively weak, compared to protein-protein interactions, but is never negligible biologically, because glycans are very important molecules together with proteins and nucleic acids (van Kooyk and Rabinovich, 2008). In addition, synthetic glycans and oligosaccharides have been investigated for the detection and prevention of virus infection (Ogata et al., 2007; Schofield et al., 2007).

To analyze the binding properties of GBPs, various glycan arrays have now been developed, in which chemically synthesized glycans containing an amine or other functional group are arrayed on *N*-hydroxysuccinimide (NHS)- or epoxy-activated glass slides (Blixt et al., 2004). Such a glycan array was previously utilized as a glycan library to investigate various GBP-binding parameters (Song et al., 2008). Several glycans and oligosaccharides have been synthesized by chemical and enzymatic reactions to investigate their characteristic properties and GBP specificity (Hsu et al., 2011; Lepenies et al., 2010). In chemical synthesis of glycan, many tedious steps required to protect and deprotect hydroxyl groups (Pazynina et al., 2002; 2003) can be circumvented by stereo- and region-specific reaction by glycosyltransferases (Palcic, 2011). From a practical point, the use of glycosyltransferases is attractive for glycan synthesis, because it is highly regioselective for specific hydroxyl groups. On the other hand, glycosidases, which normally hydrolyze glycosidic bonds, catalyze two types of

reactions, transglycosylation (Yamamoto, 2013) and condensation (Yasutake et al., 2003), and the condensation reaction has been used in the synthesis of spacer-*O*-linked glycans.

In the present study, a novel P^k trisaccharide (P^k)-conjugated derivative with an alkyl spacer, a sugar unit monomer in the chemical structure, was designed and synthesized by the combination of cellulase-mediated condensation, by *Trichoderma reesei* glycosidase, and glycan transfer, using the *Neisseria gonorrhoeae* α1,4-galactosyltransferase (LgtC). This P^k would be expected to bind *E. coli* O-157 Shiga-like toxins 1a (Stx-1) and 2 (Stx-2). Shiga toxin-producing *E. coli* (STEC) produces Shiga toxin (Stx), which belongs to the AB_5 family of protein toxins, composed of one A subunit and five B subunits (Bergan et al., 2012). The A subunit has RNA *N*-glycosidase activity that causes cell death by inhibiting protein synthesis. The B subunit is non-toxic and functions to bind P^k to the surface of eukaryotic cells, allowing the toxin to enter the cell. Each B subunit has three P^k-binding sites, thus totaling 15 P^k binding sites per Stx molecule. We showed that this monovalent P^k-derivative, conjugated with a pentylamino group, showed strong binding activity to both Stx-1 and Stx-2, and thus represents a promising new candidate Stx-neutralizing agent.

2. Materials and methods

2.1. Expression of N. gonorrhoeae LgtC and Stxs B subunits

A partially deleted *lgtC* gene (1–858 bp) of *N. gonorrhoeae* F62 was synthesized by Eurofins MWG Operon (Tokyo, Japan). This synthesized *lgtC* gene was codon-

optimized for expression in *E. coli* with its C-terminal 25 amino acids deleted. To attach a spacer (GGGGSGGGGS) and 6 × His tag, the *lgtC* gene was amplified by PCR using A4GalT-frw and A4GalT-21-rev primers (Table 1). In addition, the sequence of the spacer and 6 × His tag was prepared using GS-H6 as a PCR template for GS-H6(-21)-frw and GS-H6-rev PCR primers. The *lgtC* gene attached to the spacer and 6 × His tag was PCR-amplified using the *lgtC* gene and DNA fragment of the spacer and 6 × His tag as templates and the A4GalT-frw and GS-H6-rev primers (Table 1). The amplified gene was then inserted into a pET32b vector by In-Fusion technology (CLONTECH, Mountain View, CA, USA). Linearized pET32b was prepared by PCR using pET32-frw and pET32-rev as primers. The recombinant pET32b construct was transformed into *E. coli* BL21 (DE3) cells. Expression of 6 × His-tagged LgtC was induced by the addition of 1 mM isopropyl-β-D-1-thiogalactopyranoside (IPTG) in the culture of this transformant in LB medium supplemented with 100 μg/ml of ampicillin.

DNA fragments composed of the coding sequences for the Stx1a-B and Stx2a-B subunits were synthesized by Eurofins MWG Operon, Inc. To attach the sequence of a spacer (GGGGSGGGGS) and 6 × His tag, each B subunit gene was amplified by PCR using Stx1a-B-frw and Stx1a-B-rev primers or Stx2a-B-frw and Stx2a-B-rev primers (Table 1), respectively. The sequence of the spacer and 6 × His tag was also prepared using GS-H6 as a PCR template and GS-H6-1aB-frw or GS-H6-2aB-frw and GS-H6-rev as PCR primers. The sequence containing the spacer and 6 × His tag was added to each gene by PCR, and the amplified genes inserted into pET32b vectors in the same manner as the *lgC-His* gene, using In-Fusion technology. Each constructed vector was then transformed into *E. coli* BL21 (DE3) cells, and the expression of each His-tagged

B subunit carried out in the same manner as LgtC expression.

2.2. Purification of LgtC and Stx B subunits

Purification of LgtC, Stx1a-B-His and Stx2a-B-His was performed using His60 Ni Super flow (CLONTECH) or TALON affinity gel column chromatography. Pelleted cells were suspended in 50 mM Tris-HCl (pH 7.8) containing 150 mM NaCl (Buffer A) and disrupted by sonication. The homogenate was then centrifuged at 5000 × g and the supernatant collected and loaded onto a TALON resin affinity column, and this column was washed by Buffer A containing 40 mM imidazole. Each protein was eluted with Buffer A containing 300 mM imidazole. For size-exclusion chromatography, a Superdex 200 10/300 GL column (GE Healthcare Japan, Tokyo, Japan) was used. Buffer A was used as a running buffer. One milliliter of purified Stx1a-B (0.05 mg/ml) or Stx2a-B (0.4 mg/ml) was used for this size-exclusion chromatography.

2.3. SDS-PAGE

Recombinant protein samples were subjected to SDS-PAGE on 10 or 12% polyacrylamide gels using the Mini-protean II system (Bio-Rad, Hercules, CA, USA). For Stx-Bs, Tris-Tricine SDS-PAGE was adopted. Total proteins on SDS-PAGE gels were detected by Coomassie Brilliant blue R-250 or silver staining. Protein concentrations were measured by BCA Protein Assay-Reducing Agent Compatible (Thermo Fisher Scientific, Rockford, IL, USA).

2.4. 5-Trifluoroacetamido-1-pentanol (TFAP)-linked P^k (TFAP-P^k) synthesis

Synthesis of TFAP-P^k was carried out according to the scheme in Fig. 1. 5-

Trifluoroacetamidopentyl β-lactoside (TFAP-Lac) was prepared by a protocol described previously (Ogata et al., 2007). TFAP-Lac (40 mg, 0.076 mmol) and UDP-Gal (94 mg, 0.15 mmol) were first dissolved in a solution that contained 10.3 ml of 50 mM Tris-HCl (pH 6.8), $MnCl_2$ (34.6 mg), and BSA (15.3 mg), and 15.5 U (5 ml) of purified LgtC was then added. The mixture was then incubated for 4 h at 37°C, and the reaction terminated by boiling for 5 min. The supernatant was isolated by centrifugation (8000 × *g*, 20 min), concentrated and dissolved in 5 ml of $CHCl_3/CH_3OH/H_2O$ (6:4:1), and loaded onto a Silica Gel 60 N column (4.5 × 30 cm). The same solvent at a flow rate of 10 ml/min was used as a running buffer and fraction sizes of 20 ml/tube. Aliquots from fractions 17–26 were then concentrated, dissolved in 2 ml of 20% methanol, and loaded onto an ODS column (2.5 × 30 cm) equilibrated with 20% methanol, at a flow rate of 2.0 ml/min. After washing the column with 280 ml of 20% methanol, the absorbed material was eluted with 40% methanol and a fraction size of 10 ml. The absorbance of the eluate was monitored at 210 nm. An aliquot from pooled fractions 3–4 was concentrated by evaporation and lyophilized. High resolution electrospray ionization mass spectrometry (HR-ESI-MS): *m/z* 708.23174 $[M+Na]^+$ (calcd for $C_{25}H_{42}F_3N_1NaO_{17}$, 708.23025); ^1H NMR (D_2O, 500 MHz): δ 4.84 (d, 1H, $J_{1'',2''}$ 4.0 Hz, H-1''), 4.40 (d, 1H, $J_{1',2'}$ 8.0 Hz, H-1'), 4.37 (d, 1H, $J_{1,2}$ 8.0 Hz, H-1), 4.25 (1H, H-5''), 3.93-3.45 (18H), 3.23 (2H, H-ε), 3.19 (1H, H-2), 1.55 (2H, H-β), 1.51 (2H, H-δ), 1.30 (2H, H-γ); ^{13}C NMR (D_2O, 125 MHz): δ 158.9 ($CF_3\underline{C}ONH$-), 116.0 ($\underline{C}F_3CONH$-), 103.3 (C-1'), 102.0 (C-1), 100.4 (C-1''), 78.8 (C-4), 77.4 (C-4'), 75.5 (C-5'), 74.9 (C-5), 74.6 (C-3), 73.0 (C-2), 72.2 (C-3'), 71.0 (C-5''), 70.9 (C-2'), 70.4 (C-α), 69.2 (C-3''), 69.0 (C-4''), 68.6 (C-2''), 60.6 (C-6''), 60.4 (C-6'),

60.1 (C-6), 39.7 (C-ε), 28.3 (C-β), 27.5 (C-δ), and 27.5 (C-γ).

2.5. Surface plasmon resonance (SPR)

SPR analyses were performed using Biacore 2000 (GE Healthcare Japan, Tokyo, Japan). TFAP-P^k was treated with NaOH to remove trifluoroacetic acid (TFA) from amino groups and neutralized with HCl. The P^k was then immobilized onto a CM5 sensor chip (GE Healthcare Japan) by amine coupling at pH 4.0 (1500 – 2000 RU). Stx1a-B or Stx2a-B were then injected into the sensor chip in HBS-EP buffer (10 mM HEPES, 150 mM NaCl, 3 mM EDTA, 0.005% Surfactant P-20 [GE Healthcare Japan], pH 7.4) at 30 μl/min. As a regeneration buffer, 10 mM 5-aminopentyl β-P^k (AP-P^k) treated with NaOH was used. Kinetics analysis was performed using 1:1 Langmuir binding model using BIAevaluation software (GE Healthcare Japan).

2.6. Analytical methods

The α1,4-Galactosyltransferase (α1,4GalT) activity of LgtC was assayed as follows. UDP-galactose (UDP-Gal, gifted from Yamasa Corp, Chiba, Japan) (10 mM), 2-[5'-dimethylaminonaphthalene-1'-sulfonyl-(2-aminoethoxy)]ethyl β-lactoside (dansyl-Lac, 5 mM), $MnCl_2$ (12.5 mM) and BSA (1 mg/ml) were dissolved in 50 mM Tris-HCl (pH 6.8), followed by the addition of 100 μl of enzyme solution (total volume 286 μl). Dansyl-Lac was prepared as described previously (Ogata et al., 2010). The reaction was initiated 37ºC by addition of 100 μl enzyme solution (final concentration: 0.46 mg/ml of purified LgtC). At each sample time, 10 μl of the reaction mixture was added to 190 μl distilled water, followed by immediate boiling for 5 min. After

filtration through a 0.45-μm nitrocellulose filter (Millipore, Bedford, MA), the filtrates were analyzed by HPLC (Jasco LC-2000, Jasco Ltd., Tokyo, Japan) plus fluorescence detector (excitation, 330 nm; emission, 520 nm) (JOEL Ltd., Tokyo, Japan) using a Unison US-C18 (ODS, 4.6 × 250 mm, Imtakt, Japan) column, and eluted with 25% acetonitrile. The HPLC was operated isocratically at a flow rate of 1.0 ml/min and a column temperature of 40ºC. One unit of enzyme activity was defined as the amount of enzyme capable of catalyzing the transfer of 1 μmol of Gal per minute.

Electrospray ionization (ESI) mass spectra were measured by a JMS-T100LC mass spectrometer (JOEL). 500-MHz ^{1}H NMR spectra and 125-MHz ^{13}C NMR spectra were recorded using a JNM-ECX500II spectrometer (JOEL). Chemical shifts were expressed in ppm relative to the methyl resonance of the external standard sodium 3-(trimethylsilyl) propionate.

3. Results and discussion

3.1. Expression and purification of LgtC

LgtC was expressed in the soluble fraction in *E. coli* and purified by His60 Ni Super flow column chromatography with 300 mM imidazole. Purified LgtC was observed as a single band on an SDS-PAGE gel (Fig. 2A), corresponding to its molecular weight estimated from its amino acid sequence. α4GnT activity of LgtC was detected using Dansyl-Lac and UDP-Gal as substrate in both cell homogenates (Fig. 2B) and purified samples (Fig. 2C) also, indicating that active α4GnT was expressed. Expressed LgtC in *E. coli* was 13-fold purified from the crude extract and finally, 0.14

192 mg of purified LgtC was obtained from 100 ml *E. coli* culture (Table 2). The specific
193 activity of this purified LgtC was 66 U/mg, 13-fold higher than that of *N. meningitidis*
194 LgtC purified from *E. coli* (Zhang et al., 2002). In the study of *N. meningitidis* LgtC,
195 UDP-D-[6-^{3}H] galactose and lactose were used for α4GnT assay as a sugar donor and
196 acceptor**,** different from the substrates used in this study. This difference may cause
197 discrepancies between the specific activity of the *N. gonorrhoeae* LgtC (used here) and
198 that of *N. meningitidis* LgtC. Optimal pH and temperature in this assay were 8.0 and
199 40°C, respectively (Fig. 3).

200 *3.2. TFAP-P^{k} synthesis*

201 A condensation reaction between lactose and TFAP was first catalyzed by cellulase
202 from *T. reesei* to obtain TFAP-Lac, as described in our previous report (Ogata et al.,
203 2007). In this study, TFAP-lactose was obtained in 0.67% yield based on the initial
204 amount of lactose. This yield was a little lower than that (1.0%) in previous paper
205 (Ogata et al., 2007). The efficiency of this condensation reaction by cellulase is low,
206 but this reaction is an easy way to provide β-glycoside stereo-specifically, because it
207 does not require any protection and deprotection steps. A novel *O*-linked P^{k}-conjugated
208 derivative with an alkyl spacer was then derived from the resulting product utilizing
209 the above-described purified LgtC (Fig. 1). The yield of this reaction was 67% based
210 on the initial amount of TFAP-lactose. Addition of α1,4-linked Gal to the TFAP-Lac
211 acceptor led to the synthesis of trisaccharide glycoside TFAP-P^{k}. Synthesized TFAP-P^{k}
212 was purified by Silica Gel 60 N column and ODS column (Fig. 4A) and HR-ESI-MS
213 analysis of synthesized TFAP-P^{k} showed [M + Na^{+}] ion at *m/z* 708.23174,
214 corresponding to the molecular formula, $C_{25}H_{42}F_3N_1NaO_{17}$ (calcd, 708.23025) (Fig.

3B). In addition, ^{1}H NMR spectroscopy was performed to confirm the structure of synthesized TFAP-P^k. LgtC purified from *E. coli* catalyzed the addition of galactose to TFAP-N-acetyllactosamine (Fig. 5). In a previous study, lactosyl-ceramide was galactosylated by catalytical reaction at the terminal Gal residue to obtain P^k-ceramide using α4GalT from *N. meningitidis* (Adlercreutz et al., 2010). However, no additional transfer of galactose to TFAP-P^k was observed here, using LgtC from *N. gonorrhoeae* for a 4-h reaction, indicating that *N. gonorrhoeae* LgtC has more narrow substrate specificity for P^k synthesis than α4GalT from *N. meningitidis.* In this point, LgtC from *N. gonorrhoeae* is more feasible for P^k synthesis than α4GalT from *N. meningitidis.*

3.3. Expression and purification of Stxs B subunits

Stx1a-B and Stx2a-B were expressed in *E. coli* and purified using TALON affinity gel chromatography. By SDS-PAGE, purified Stx1a-B and Stx2a-B were observed to be close to their estimated molecular weights (Fig. 6A). MALDI-TOF MS revealed the molecular weights of Stx1a-B and Stx2a-B to be 9139 Da and 8950 Da, respectively. This result indicates that the native signal peptide of each B subunit was cleaved off (1–20 aa of Stx1a-B and 1–19 aa of Stx2a-B), and each subunit might be secreted to the periplasm. By SDS-PAGE, each protein band was observed to be over 10 kDa, despite the exact molecular weight of both B subunits being below 10 kDa. This discrepancy may be caused by the 6 × His tag slowing protein mobility through SDS-PAGE, due to its positive charge. In gel filtration chromatography, each peak (Stx1a-B and Stx2a-B) was observed at around 20 and 30 kDa (Fig. 6B), respectively, indicating that these Stxs-B were expressed and purified as a dimer or trimer at 0.3 mM, and not as a pentamer. In the range of 5 to 85 μM, recombinant Stx1a-B produced in *E. coli*

entirely formed pentamers, and recombinant Stx2a-B produced in *E. coli* existed predominantly as pentamers at more than 50 μM (Kitova et al., 2005). In another report, both recombinant subunits were expressed in *E. coli* as pentamers (Conrady et al., 2010). In the current study, a 6 × His tag was attached to the C-terminus of each B subunit. These results suggest that the 6 × His tag may prevent both B subunits from forming pentamers.

3.4. P^k binding of Stx B subunits

The synthesized TFAP-P^k was deacylated to AP-P^k by alkali treatment. AP-P^k was then immobilized on a CM5 chip by amine coupling, and various concentrations of each B subunit were then applied to the CM5 chip. The K_D of each B subunit was calculated by BIAevaluation software using obtained sensorgrams. Specific binding of each B subunit was observed to TFAP-P^k immobilized on the CM5 chip (Fig. 7), and each B subunit was washed out by free TFAP-P^k. The K_Ds of Stx1a-B and Stx2a-B were 6.8×10^{-6} M ($k_{on} = 4.1 \times 10^{1}$ $M^{-1}S^{-1}$, $k_{off} = 2.8 \times 10^{-4}$ S^{-1}) and 2.2×10^{-5} M ($k_{on} = 3.9 \times 10^{2}$ $M^{-1}S^{-1}$, $k_{off} = 8.6 \times 10^{-3}$ S^{-1}), respectively. Soltyk et al. reported that the K_D of the Stx1 B subunit pentamer to P^k was 4.8×10^{-3} M when immobilized on a CM5 sensor chip, as determined by SPR (Soltyk et al., 2002). Here, SPR determinations of k_{on} and k_{off} were impossible because the rapid kinetics of association and dissociation of the P^k ligand was observed. However, the K_D of the same Stx1 B subunit pentamer to P^k was previously reported to be 3×10^{-9} M ($k_{on} = 2 \times 10^{5}$ $M^{-1}S^{-1}$, $k_{off} = 6 \times 10^{-4}$ S^{-1}) when P^k incorporated into liposomes containing *Salmonella* serogroup B lipopolysaccharide was immobilized on a CM5 sensor chip (Soltyk et al., 2002). Thus theoretically, SPR in this study would be the same as the later experiment, in view of

261 the immobilization of P^k on the CM5 sensor chip, although the K_D of the Stx1 B
262 subunit pentamer in the previous paper (3×10^{-9} M) was >1000-fold smaller than that
263 of the Stx1a-B dimer used in this study (5.2×10^{-6} M). This difference might be caused
264 by the subunit state of Stx1a-B, pentamer or dimer. However, k_{off} of the B subunit
265 pentamer in the previous paper ($k_{off} = 6 \times 10^{-4}$ S^{-1}) is comparable to that of the Stx1a-B
266 dimer of this study ($k_{off} = 2.4 \times 10^{-4}$ S^{-1}), indicating that the subunit state of the Stx B
267 subunit is not involved in its dissociation from the P^k ligand but instead, has crucial
268 effects on its ligand association (k_{on}). The K_D of the Stx B subunit to P^k-Cer-displaying
269 cells was 10^{-8} – 10^{-9} M (Fuchs et al., 1986). These results showed that immobilization
270 of the P^k ligand on the sensor chip is favorable for kinetic analysis of the Stx B subunit,
271 and synthesis of the spacer-linked sugar chain is amenable to binding analysis of
272 glycan-binding proteins and further development of an Stx-neutralizing agent.
273 However, in this biacore analysis, 1:1 Langmuir binding model fitting was adopted in
274 spite of three P^k binding sites of Stx B subunits. 1:1 Langmuir binding model fitted the
275 sensorgrams with low value of χ^2, 7.79 and 6.79 for Stx1 B subunit and Stx2 B
276 subunit, respectively. However this fitting model limits the detailed binding analysis of
277 the multivalency of Stx B subunits. If an isothermal titration calorimetry was used for
278 binding analysis of multivalency of Stx B subunits, highly accurate data would be
279 obtained.

280 In this study, we performed successfully novel enzymatic synthesis of spacer-
281 linked P^k trisaccharide (TFAP- P^k) by cellulose from *T. reesei* and recombinant LgtC of
282 *N. meningitides* purified from *E. coli*. The TFAP-P^k was utilized for the binding assay
283 of recombinant Stx B subunits to P^k by SPR experiment. This cellulase-mediated

condensation from cellulase and glycosyltransferase is a valuable tool for the synthesis of spacer-linked oligosaccharide.

Acknowledgement

This work was supported partly by Promotion of Nanobio-Technology Research to support Aging and Welfare Society from the Ministry of Education, Culture, Sports, Science and Technology, Japan. There was no additional external funding received for this study.

References

Adlercreutz, D., Weadge, J.T., Petersen, B.O., Duus, J.Ø., Dovichi, N.J., Palacic, M.M., 2010. Enzymatic synthesis of Gb3 and iGb3 ceramides. Carbohydrate Research 345, 1384–1388.

Bergan, J., Lingelem, A.B.D., Simm, R., Skotland, T., Sandvig, K., 2012. Shiga toxins. Toxicon 60, 1085–1107.

Blixt, O., Head, S., Mondala, T., Scanlan, C., Hufletjt, M.E., Alvarez, R., Bryan, M.C., Fazio, F., Calarese, D., Stevens, J., Razi, N., Stevens, D.J., Skehel, J.J., van Die, I., Burton, D.R., Wilson, I.A., Cummings, R., Bovin, N., Wong, C.H., Paulson, J.C., 2004. Printed covalent glycan array for ligand profiling of diverse glycan binding proteins. Proceedings of the National Academy Sciences USA 101, 17033–17038.

Conrady, D.G., Flagler, M.J., Friedmann, D.R., vander Wielen, B.D., Kovall, R.A., Weiss, A.A., Herr, A.B., 2010. Molecular basis of differential B-pentamer stability of Shiga toxins 1 and 2. PLoS One 5: e15153.

Fuchs, G., Mobassaleh, M., Donohue-Rolfe, A., Montgomery, R.K., Grand, R.J., Keusch, G.T., 1986. Pathogenesis of *Shigella diarrhea*: rabbit intestinal cell microvillus membrane binding ite for Shigella toxin. Infection and Immunity 53, 372–377.

Hsu, C.H., Hung, S.C., Wu, C.Y., Wong, C.H., 2011. Toward automated oligosaccharide synthesis. Angewandte Chemie- International Edition 50, 11872–11923.

Kitova, E.N., Daneshfar, R., Marcato, P., Mulvey, G.L., Armstrong, G., Klassen, J.S., 2005. Stability of the homopentameric B subunits of Shiga toxins 1 and 2 in solution and the gas phase as revealed by nanoelectrosprayfourier transform iron cyclotron resonance mass spectrometry. Journal of American Society of Spectrometry 16, 1957–1968.

Lepenies, B., Yin, J., Seeberger, P.H., 2010. Applications of synthetic carbohydrates to chemical biology. Current Opinion in Chemical Biology 14, 404–411.

Ogata, M., Murata, T., Murakami, K., Suzuki, T., Hidari, K.I.P.J., Suzuki, Y., Usui, T., 2007. Chemoenzymatic synthesis of artificial glycopolypeptides containing multivalent sialyloligosaccharides with a γ-polyglutamic acid backbone and their effect on inhibition of infection by influenza viruses. Bioorganic Medicinal Chemistry 15, 1383–1393.

Ogata, M., Obara, T., Chuma, Y., Murata, T., Park, E.Y., Usui, T., 2010. Molecular design of fluorescent labeled glycosides as acceptor substrates for sialyltransferases. Bioscience Biotechnology and Biochemistry 74, 2287–2292.

Palcic, M.M., 2011. Glycosyltransferases as biocatalysts. Current Opinion in Chemical Biology 15, 226–233.

329 Pazynina, G.V., Sablina, M.A., Tuzikov, A.B., Chinarev, A.A., Bovin, N., 2003.
330 Synthesis of complex α2,3-sialooligosaccharides, including sulfated and
331 fucosylated ones, using Neu5Acα2-3Gal as a building block. Mendeleev
332 Communications 13, 245–248.
333 Pazynina, G.V., Severov, V.V., Bovin, N., 2002. Synthesis of N-acetyllactosamine-
334 terminated oligosaccharides-fragments of glycanprotein O-chains. Mendeleev
335 Communications 12, 183–184.
336 Schofield, C.L., Field, R.A., Russell, D.A., 2007. Glyconanoparticles for the
337 colorimetric detection of cholera toxin. Analytical Chemistry 79, 1356–1361.
338 Soltyk, A.M., MacKenzie, C.R., Wolski, V.M., Hirama, T., Kitov, P.I., Bundle, D.R.,
339 Brunton, J.L., 2002. A mutational analysis of the globotriaosylceramide-binding
340 sites of verotoxin VT1. Journal of Biological Chemistry 277, 5351–5359.
341 Song, X., Xia, B., Lasanajak, Y., Smith, D.F., Cummings, R.D., 2008. Quantifiable
342 fluorescent glycan microarrays. Glycoconjugate Journal 25, 15–25.
343 van Kooyk, Y., Rabinovich, G.A., 2008. Protein-glycan interactions in the control of
344 innate and adaptive immune responses. Nature Immunology 9, 593–601.
345 Yamamoto, K., 2013. Recent advances in glycotechnology for glycoconjugate
346 synthesis using microbial endoglycosidases. Biotechnoloy Letter 35, 1733–1743.
347 Yasutake, N., Totani, K., Harada, Y., Haraguchi, S., Murata, T., Usui, T., 2003.
348 Efficient synthesis of glycerol β-lactoside and its derivatives through a
349 condensation reaction by cellulase. Biochimica et Biophysica Acta 1620, 252–258.
350 Zhang, J., Kowal, P., Fang, J., Andreana, F., Wang, P.G., 2002. Efficient
351 chemoenzymatic synthesis of globotriose and its derivatives with a recombinant a-
352 (1→4)-galactosyltransferase. Carbohydrate Research 337, 969–976.

353 **Table 1.** Primers and His-tag template.

Name	5’ – 3’
A4GalT-frw	GAAGGAGATATACATGGACATCGTCTTTGCTGC
A4GalT-21-rev	GAGCCACCGCCACCCGGAGGAACAGCCAGTTTCC
GS-H6-(-21)-frw	GGAAACTGGCTGTTCCTCCGGGTGGCGGTGGCTC
GS-H6-rev	CGCAAGCTTGTCGACTTAGTGGTGATGGTGATGATG
pET32-frw	ATGTATATCTCCTTCTTAAAGTTAAACAAAATTATTTC
pET32-rev	GTCGACAAGCTTGCGGC
Stx1a-B-frw	GAAGGAGATATACATGAAAAAAACATTATTAATAGCTGC
Stx1a-B-rev	GAGCCACCGCCACCACGAAAAATAACTTCGCTGAATC
GS-H6-B1a-frw	GATTCAGCGAAGTTATTTTTCGTGGTGGCGGTGGCTC
Stx2a-B-frw	GAAGGAGATATACATGAAGAAGATGTTTATGGCGG
Stx2a-B-rev	GAGCCACCGCCACCGTCATTATTAAACTGCACTTCAGC
GS-H6-B2a-frw	GCTGAAGTGCAGTTTAATAATGACGGTGGCGGTGGCTC
GS-H6 template	GGTGGCGGTGGCTCTGGAGGCGGAGGCTCACATCATCACC ATCACCACTA

354

355 **Table 2.** Purification of recombinant LgtC.

	Volume (ml)	Activity (U)	Protein (mg)	Specific activity (U/mg)	Yield (%)	Purification (Fold)
Crude	2.5	52	11	5.0	100	1
Elution	2	9.3	0.14	66	18	13

356

357

Figure legends

Fig. 1. Scheme of enzymatic synthesis of TFAP-P^k.

Fig. 2. Purification and characterization of recombinant LgtC. (A) SDS-PAGE of purified recombinant LgtC. Lane 1: molecular weight marker, lane 2: cell homogenate, lane 3: purified LgtC. (B) HPLC chromatograms of LgtC reaction mixtures using cell homogenate. (C) Time course of the production of Dansyl-P^k from Dansy-Lac using purified recombinant LgtC.

Fig. 3. Characterization of recombinant LgtC. (A) Optimal pH of recombinant LgtC. The activity was measured in each pH condition prepared by indicated buffers. (B) Optimal temperature of recombinant LgtC. The assay was performed at each temperature.

Fig. 4. Synthesis of TFAP-P^k. (A) Chromatogram of ODS column chromatography for the purification of TFAP-P^k. TFAP-P^k was eluted by 40% methanol. (B) HR-ESI-MS analysis of synthesized TFAP-P^k.

Fig. 5. 500 MHz ^{1}H NMR spectrum of TFAP-P^k. Solvent, D_2O; temperature, 25ºC; concentration, 8.3 mg/ml.

Fig. 6. Purification of recombinant Stx1a-B and Stx2a-B. (A) SDS-PAGE of Stx1a-B and Stx2a-B purified by TALON affinity gel column chromatography. Lane 1: molecular weight marker, lane 2: cell homogenate, Lane 3: wash fraction 1, lane 4: wash fraction 2, lane 5: elution fraction. (B) Chromatograms of Superdex 200 10/300 GL column chromatography using one milliliter of purified Stx1a-B (0.05 mg/ml) and

379 Stx2a-B (0.4 mg/ml). To estimate molecular weight of each purified protein, Gel
380 filtration calibration kit (Low molecular weight, GE Healthcare Japan) was used. This
381 kit contains Conalbumin (75 kDa), Ovalbumin (44 kDa), Carbonic anhydrase (29
382 kDa), Ribonuclease (13.7 kDa) and Aprotinin (6.5 kDa).

383 **Fig. 7.** Sensorgrams of SPR experiment using purified Stx1a-B and Stx2a-B. This SPR
384 experiment was performed using Biacore 2000. TFAP-P^k treated with NaOH was
385 immobilized on the CM5 sensor chip and each concentration of purified Stx1a-B or
386 Stx2a-B was injected into the sensor. As a regeneration buffer, 10 mM TFAP-P^k treated
387 with NaOH was used.

Figure 1, Kato et al.

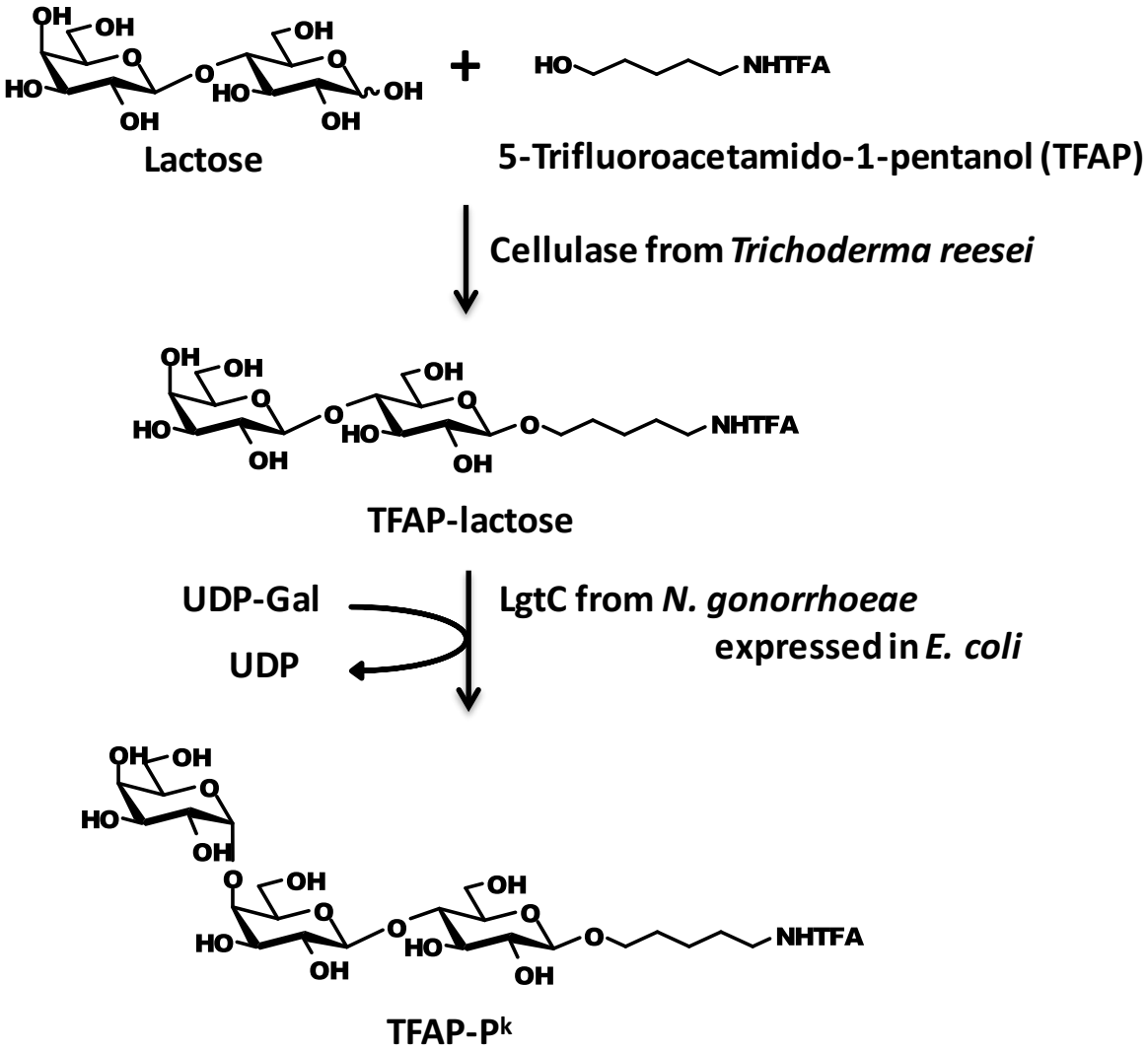

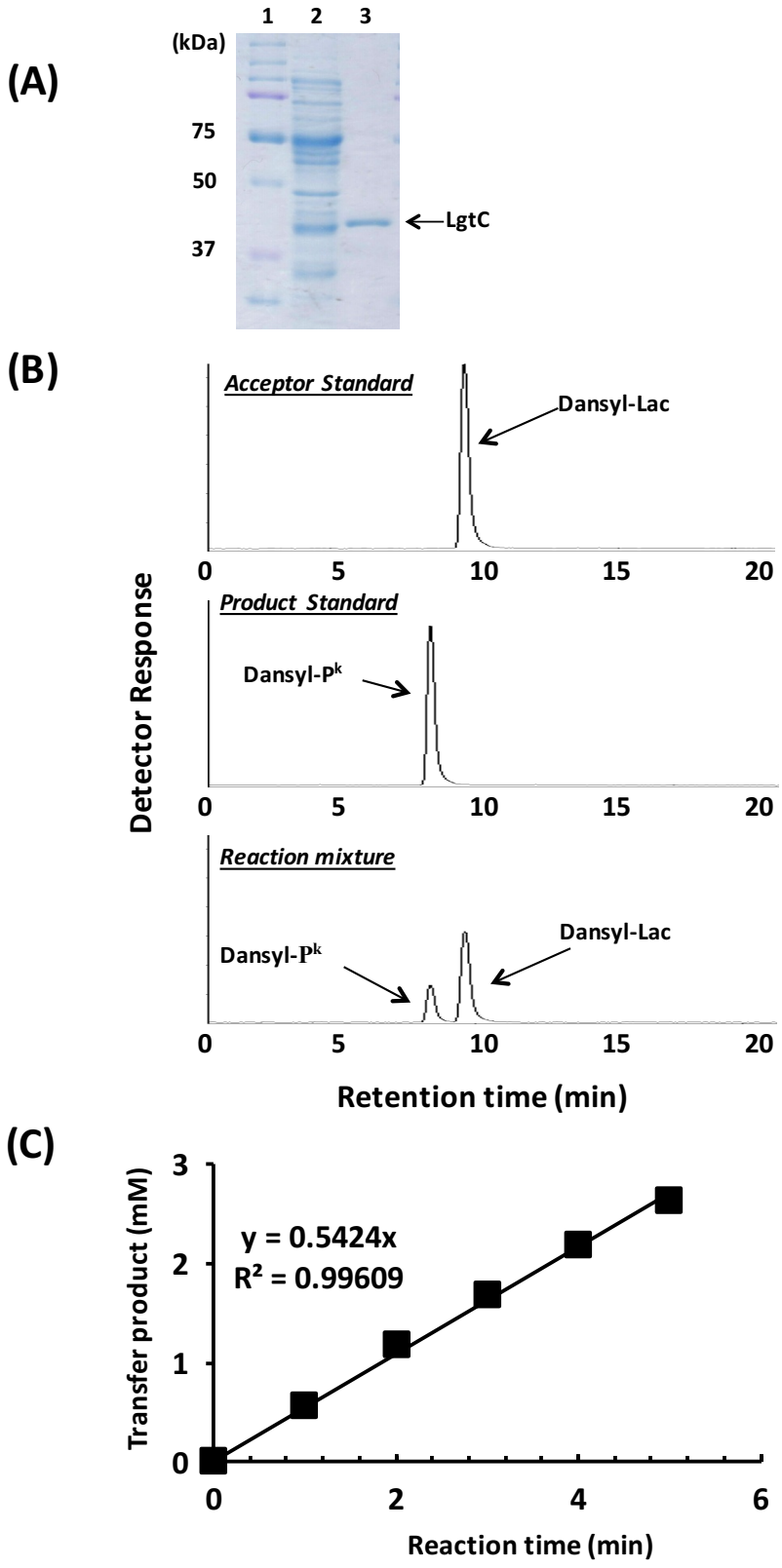
(A)
1 2 3
(kDa)
75
50
37
LgtC
(B)
Acceptor Standard
Dansyl-Lac
Product Standard
Dansyl-P^k
Reaction mixture
Dansyl-P^k
Dansyl-Lac
0 5 10 15 20
Detector Response
Retention time (min)
(C)
y = 0.5424x
R² = 0.99609
Transfer product (mM)
0 1 2 3
0 2 4 6
Reaction time (min)

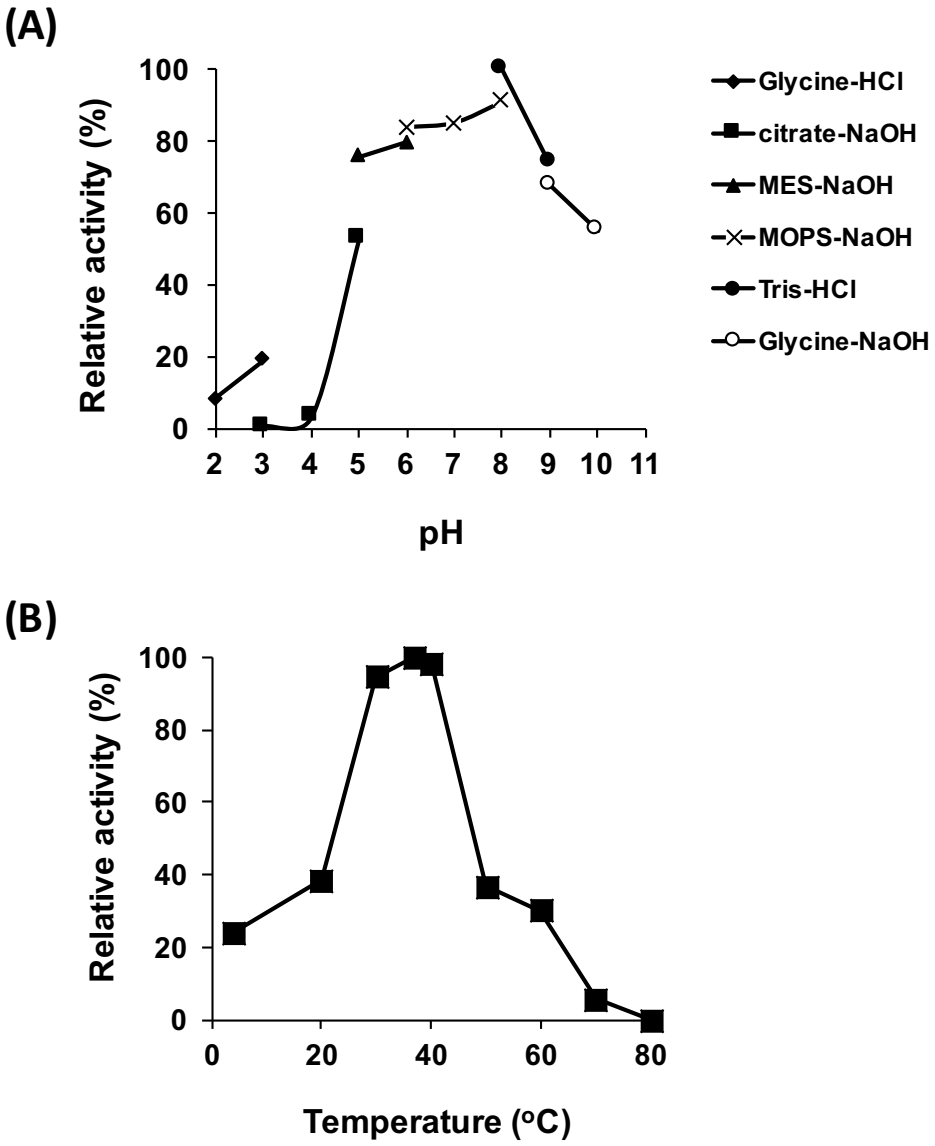
(A)
Relative activity (%)
100
80
60
40
20
0
2 3 4 5 6 7 8 9 10 11
pH
Glycine-HCl
citrate-NaOH
MES-NaOH
MOPS-NaOH
Tris-HCl
Glycine-NaOH
(B)
Relative activity (%)
100
80
60
40
20
0
0 20 40 60 80
Temperature (°C)

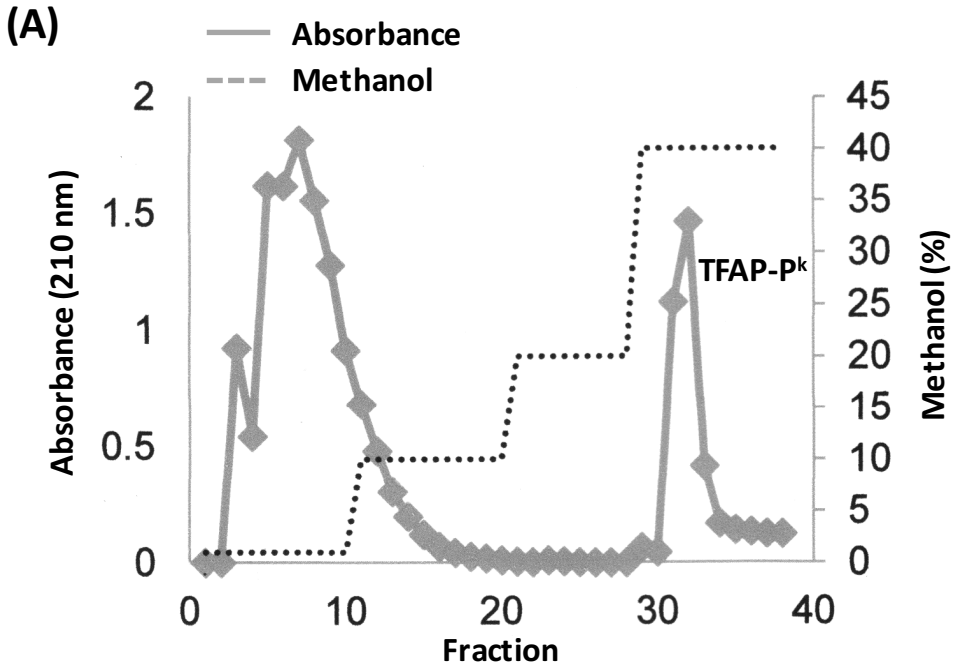
(A)
Absorbance
Methanol
Absorbance (210 nm)
Methanol (%)
TFAP-P^k
Fraction
0
10
20
30
40
0
0.5
1
1.5
2
0
5
10
15
20
25
30
35
40
45

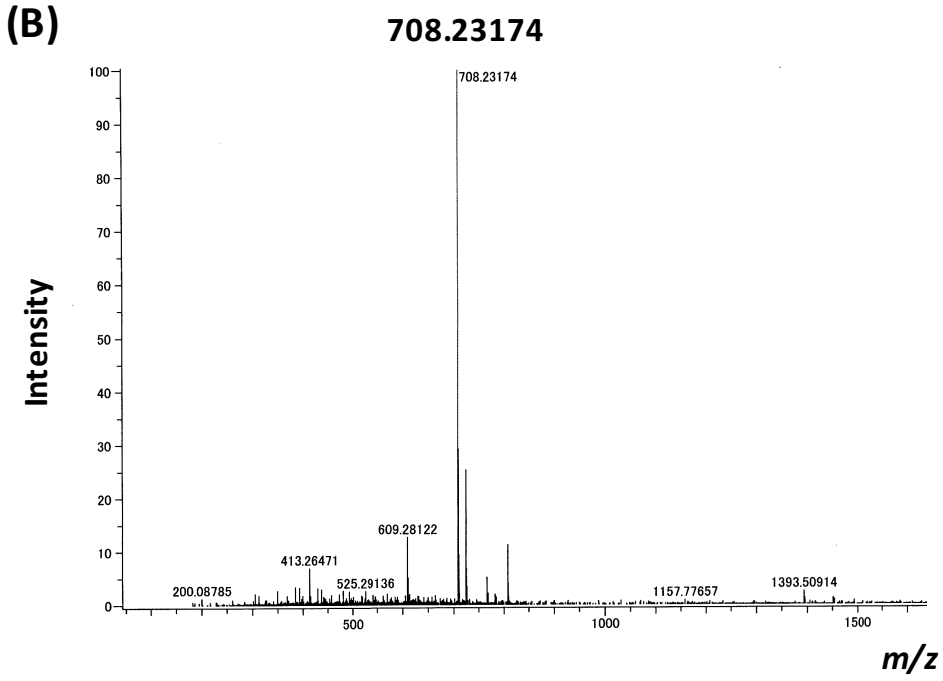
(B)
708.23174
Intensity
m/z
708.23174
609.28122
413.26471
525.29136
200.08785
1157.77657
1393.50914
500
1000
1500

Figure 5, Kato et al.

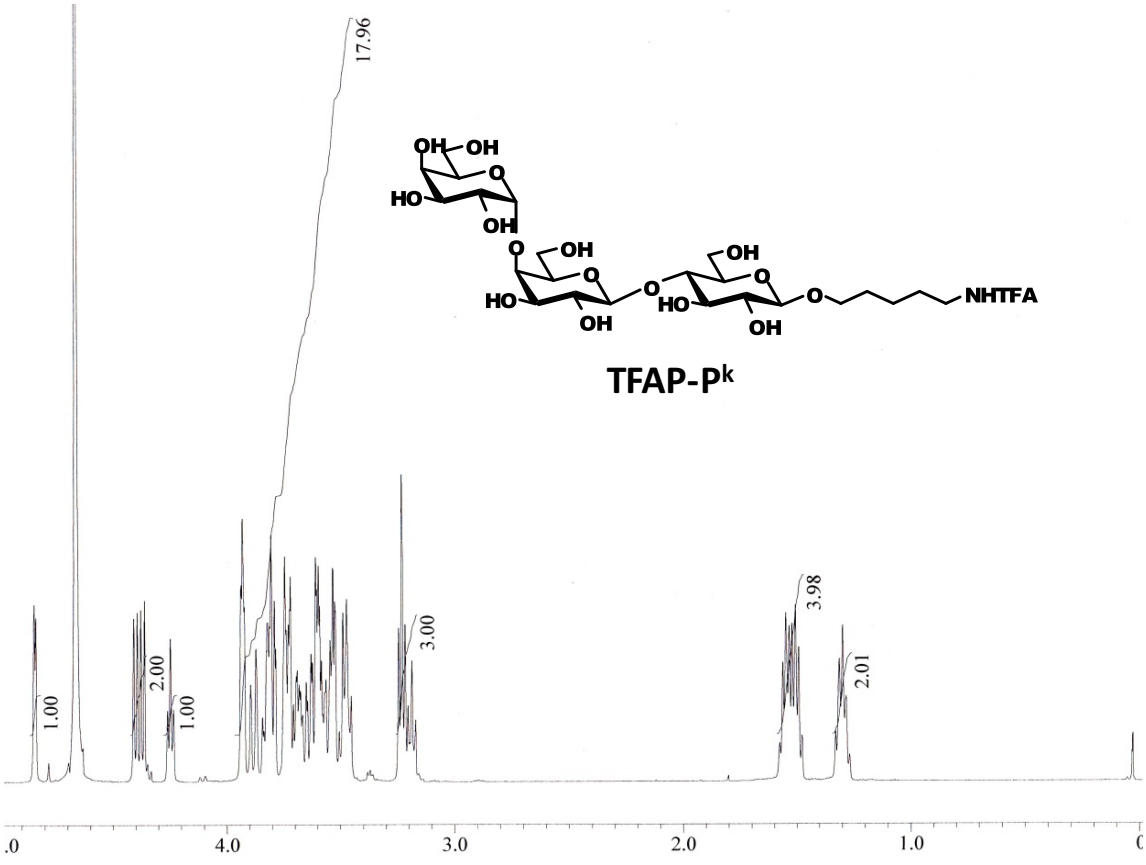

TFAP-P^{k}

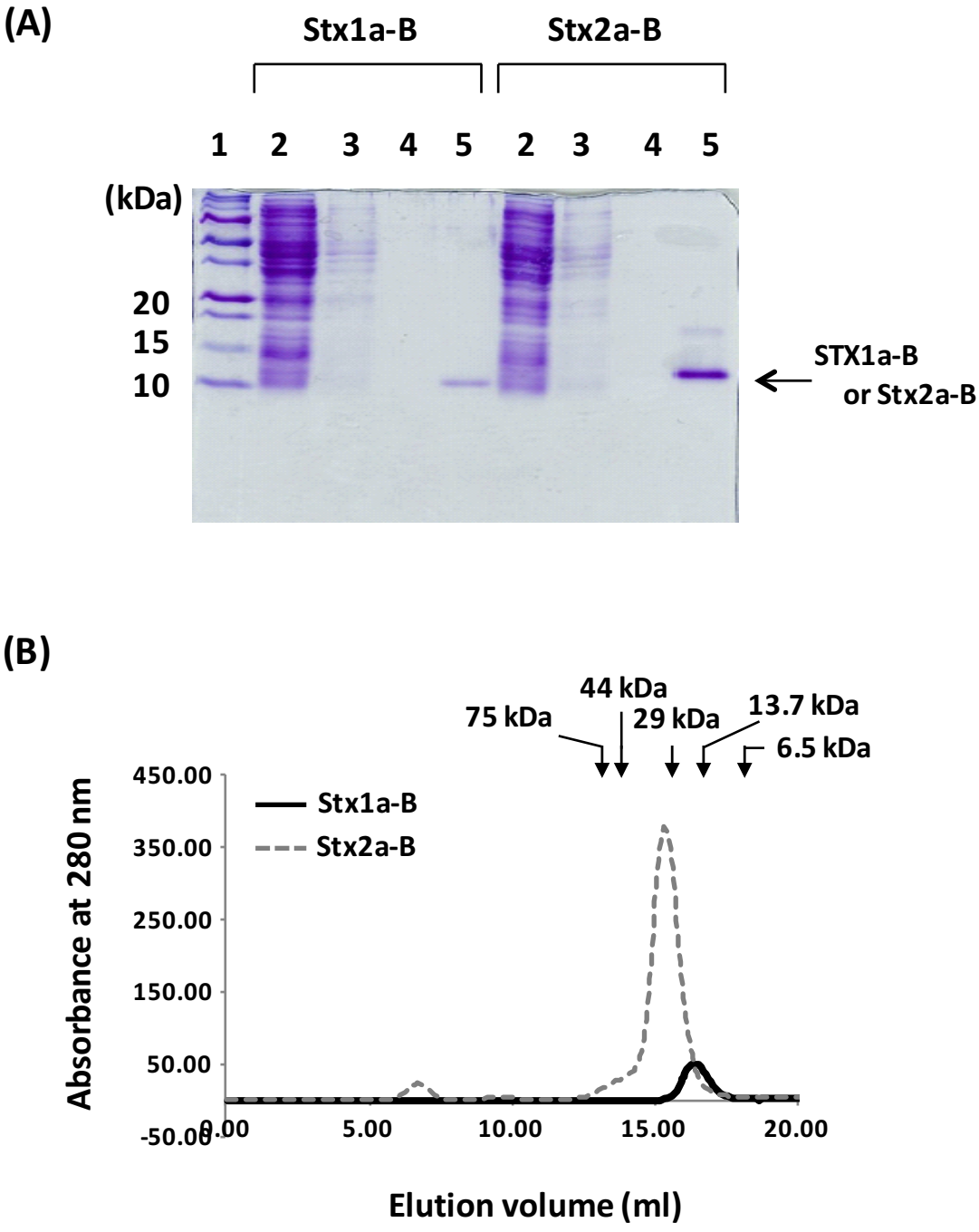
(A)
Stx1a-B
Stx2a-B
1 2 3 4 5 2 3 4 5
(kDa)
20
15
10
STX1a-B
or Stx2a-B
(B)
75 kDa
44 kDa
29 kDa
13.7 kDa
6.5 kDa
Stx1a-B
Stx2a-B
Absorbance at 280 nm
450.00
350.00
250.00
150.00
50.00
-50.00
0.00
5.00
10.00
15.00
20.00
Elution volume (ml)

Figure 7, Kato et al.